



DESIGNING, BUILDING AND VALIDATING A TEST RIG TO MEASURE TWO-PORT DATA OF SMALL FANS

Emil GARNELL¹, Mats ÅBOM¹, Guy BANWELL²

¹ *MWL, KTH Royal Institute of Technology, SE-100 44, Stockholm, Sweden*

² *DYSON, Tetbury Hill, Malmesbury SN16 0RP, United Kingdom*

SUMMARY

One way to obtain a complete description of a sound source in a duct is to measure two-port data, comprising of the source scattering matrix and the source cross-spectrum. The present paper offers a review of the main guidelines for designing and building a two-port rig to measure high speed small fans, as well as an example of how this data can be used.

The standard method that is most widely used nowadays to derive the source cross-spectrum is shown to become singular when the reflection coefficients at the rig terminations are high. A new post-processing method is suggested and tested against the standard one. It is shown to behave better in highly reflective cases, but is more sensitive to flow noise.

INTRODUCTION

Everyday household appliances are known to be noisy: vacuum cleaners, hand dryers, hair dryers... All these examples are fluid machines, that contain a fan that compresses the air and generates flow. In view of noise control, the most important part of these machines is the sound source, that is to say the rotating fan. Characterization of the source is the start for efficient noise control.

The simplest characterization of a source in a duct is to measure the radiated sound power. This method has been widely used and is described in an ISO standard [1]. However, the radiated power depends not only on the source, but also on the rest of the machine (boundary conditions, mounting...). Therefore a more complete characterization of the source is necessary to be able to predict the acoustic behaviour of the source in an arbitrary geometry. The 2-port formulation allows to model all passive elements of a duct system by a 2x2 matrix, and all active elements by a 2x2 matrix plus a source vector [2]. The complete duct system is then modelled by connecting the element matrices together. Any element matrix is independent of its surroundings, so this formalism can be used to describe any duct system.

TWO-PORT MEASUREMENT METHODS

Literature review

A two-port is a black box, that enforces a linear relationship between two inputs and two outputs. It can be described in different formalisms: the transfer matrix formalism is well suited to study duct assemblies with a main propagation direction, but the modelling of complex networks including source term is quite inconvenient. Glav and Åbom argued that another formalism, based on the travelling wave amplitudes, is more suitable to study complex networks with source-terms [3]. The state variables used to describe an active two-port in the scattering formalism are defined in Fig 1.

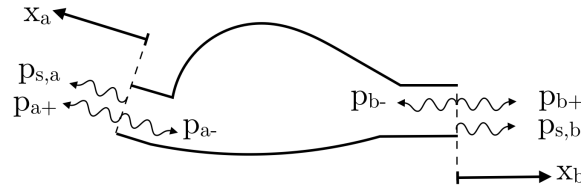


Figure 1: Definition of the state variables for the scattering matrix formalism, where a denotes the inlet side and b the outlet side.

The scattering matrix S , the source vector p_s and the source cross-spectrum G_s are defined as:

$$\begin{bmatrix} p_{a+} \\ p_{b+} \end{bmatrix} = \begin{bmatrix} S_{11} & S_{12} \\ S_{21} & S_{22} \end{bmatrix} \begin{bmatrix} p_{a-} \\ p_{b-} \end{bmatrix} + \begin{bmatrix} p_{s,a} \\ p_{s,b} \end{bmatrix} \quad \Leftrightarrow \quad p_+ = S p_- + p_s \quad , \quad G_s \equiv p_s p_s^\dagger \quad (1)$$

The first measurement method using modern analysers for obtaining the scattering matrix and the source vector of fans in ducts was proposed by Terao and Sekine in 1989 [4]. However, the most widely used method nowadays is the one proposed by Lavrentjev et al. in [5], because it introduces a very practical way to suppress flow noise from measurements. As flow noise is correlated only over a specific length (the correlation length [6]), it can be averaged out in cross-spectrum measurements if the distance between two microphones is large enough. Therefore, flow noise is a problem only when auto-spectra are measured. In [5] the authors show that auto-spectra can be replaced by cross-spectra, by transferring the pressure at one microphone location to another's using the transfer matrix of the duct element located between the two microphones. The method of [5] has been further improved by Holmberg in [7], where over-determination is used to compute both the scattering matrix and the source cross-spectrum matrix, to improve measurement accuracy. The method used by Holmberg is hereafter referred to as the *standard method*.

Theory for the scattering matrix measurements

In this section a quick summary of the method presented in [5] and [7] is given.

White noise or a periodic signal is played alternatively on each loudspeaker while the fan is on, and the transfer functions between the loudspeaker signal and the microphone signals are computed. Each measurement is hereafter referred to as *case i* , where i is the speaker number (see Fig. 2).

The first step of the post-processing is to compute the scattering matrix and the reflection coefficient of the rig terminations. Plane wave decomposition is performed using over-determination. The microphone pressures can be expressed in terms of the travelling wave amplitudes p_+ and p_- :

$$\begin{bmatrix} e^{-ik_+x_1} & e^{ik_-x_1} \\ e^{-ik_+x_2} & e^{ik_-x_2} \\ e^{-ik_+x_3} & e^{ik_-x_3} \end{bmatrix} \begin{bmatrix} p_+ \\ p_- \end{bmatrix} = \begin{bmatrix} p_1 \\ p_2 \\ p_3 \end{bmatrix} \quad (2)$$

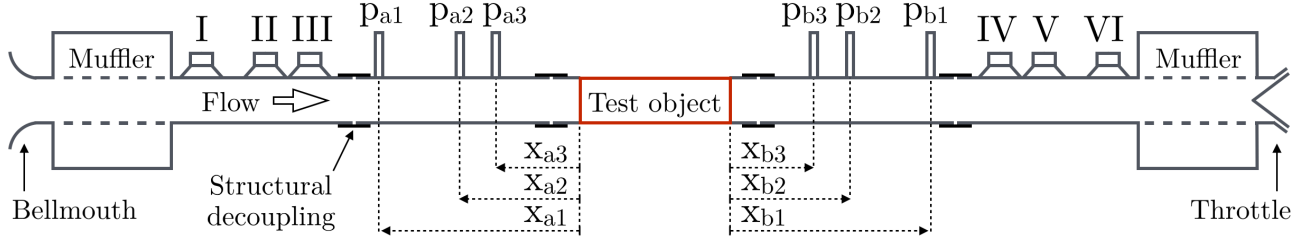


Figure 2: Schematic of the measurement rig, with definition of the measured quantities.

which can be solved using the Moore-Penrose pseudo-inverse. The wave-numbers are computed using the propagation model by Dokumaci [8], that takes into account visco-thermal losses during the propagation of plane waves in ducts with mean flow. If the microphone pressures in Eq. (2) are replaced by the transfer functions between the microphones and the loudspeaker signal, the obtained travelling wave amplitudes p_+ and p_- will not contain any contribution of the source vector \mathbf{p}_s . Indeed, the source vector \mathbf{p}_s is not correlated to the loudspeaker signal, and is suppressed from Eq. (1) if enough averages are carried out during the computation of the transfer functions. For the test case where loudspeaker I is on, Eq. (1) becomes:

$$\mathbf{p}_+^I = \mathbf{S}\mathbf{p}_-^I \quad (3)$$

As there are three speakers on each side, six independent test cases are measured, and Eq. (3) including all test cases reads:

$$[\mathbf{p}_+^I \quad \mathbf{p}_+^{II} \quad \dots \quad \mathbf{p}_+^{VI}] = \mathbf{S} [\mathbf{p}_-^I \quad \mathbf{p}_-^{II} \quad \dots \quad \mathbf{p}_-^{VI}] \quad (4)$$

Eq. (4) can be solved by the Moore-Penrose pseudo-inverse to find \mathbf{S} .

The reflection coefficients of the rig terminations, $R_a = \frac{p_{a-}}{p_{a+}}$ and $R_b = \frac{p_{b-}}{p_{b+}}$ can be obtained in a similar manner using the results of the plane wave decomposition. Only the test cases where the speakers on side A are off can be used to compute the reflection coefficient on side A, and vice versa for side B.

$$[p_{a+}^{IV} \quad p_{a+}^V \quad p_{a+}^{VI}] R_a = [p_{a-}^{IV} \quad p_{a-}^V \quad p_{a-}^{VI}] \quad [p_{b+}^I \quad p_{b+}^{II} \quad p_{b+}^{III}] R_b = [p_{b-}^I \quad p_{b-}^{II} \quad p_{b-}^{III}] \quad (5)$$

Standard method for the source cross-spectrum matrix computation

The speakers are switched off, and the cross-spectra between all microphones are measured. The equations describing the reflections at the rig terminations, the scattering at the test object, and the propagation of plane waves in the duct can be written as:

$$\mathbf{p}_- = \begin{bmatrix} R_a & 0 \\ 0 & R_b \end{bmatrix} \mathbf{p}_+ \equiv \mathbf{R}\mathbf{p}_+ \quad \mathbf{p}_+ = \mathbf{S}\mathbf{p}_- + \mathbf{p}_s \quad (6)$$

$$\begin{aligned} \begin{bmatrix} p(x_a) \\ p(x_b) \end{bmatrix} &= \begin{bmatrix} e^{-ik_a x_a} & 0 \\ 0 & e^{-ik_b x_b} \end{bmatrix} \mathbf{p}_+ + \begin{bmatrix} e^{ik_a x_a} & 0 \\ 0 & e^{ik_b x_b} \end{bmatrix} \mathbf{p}_- \\ \Leftrightarrow \mathbf{p}(\mathbf{x}) &= \mathbf{T}_+(\mathbf{x}) \mathbf{p}_+ + \mathbf{T}_-(\mathbf{x}) \mathbf{p}_- \end{aligned} \quad (7)$$

which can be rewritten into:

$$\mathbf{p}_s = (\mathbf{E} - \mathbf{S}\mathbf{R})\mathbf{p}_+ \quad \mathbf{p}(\mathbf{x}) = (\mathbf{T}_+(\mathbf{x}) + \mathbf{T}_-(\mathbf{x})\mathbf{R})\mathbf{p}_+ \quad (8)$$

and leads to:

$$\mathbf{p}_s = (\mathbf{E} - \mathbf{S}\mathbf{R})(\mathbf{T}_+(\mathbf{x}) + \mathbf{T}_-(\mathbf{x})\mathbf{R})^{-1}\mathbf{p}(\mathbf{x}) \equiv \mathbf{C}(\mathbf{x})\mathbf{p}(\mathbf{x}) \quad (9)$$

In order to use only cross-spectra, Eq. (9) is multiplied by the hermitian transpose of the same equation but obtained at another \mathbf{x} :

$$\mathbf{G}_s = \mathbf{p}_s \mathbf{p}_s^\dagger = \begin{bmatrix} G_{p_{a,s},p_{a,s}} & G_{p_{b,s},p_{a,s}} \\ G_{p_{a,s},p_{b,s}} & G_{p_{b,s},p_{b,s}} \end{bmatrix} \quad (10)$$

$$= \mathbf{C}(\mathbf{x}_1) \mathbf{p}(\mathbf{x}_1) \mathbf{p}(\mathbf{x}_2)^\dagger \mathbf{C}(\mathbf{x}_2)^\dagger = \mathbf{C}(\mathbf{x}_1) \begin{bmatrix} G_{p_a(x_{a2}),p_a(x_{a1})} & G_{p_b(x_{b2}),p_a(x_{a1})} \\ G_{p_a(x_{a2}),p_b(x_{b1})} & G_{p_b(x_{b2}),p_b(x_{b1})} \end{bmatrix} \mathbf{C}(\mathbf{x}_2)^\dagger \quad (11)$$

If there are more than two microphones on each side, Eq. (11) can also be overdetermined, see [7] for the details.

DESIGN GUIDELINES

In the present section, guidelines for the design of the different rig elements are given.

Microphones

To allow plane wave decomposition with over-determination, and to cover a wide frequency range, at least three microphones are needed on each side of the test object. The spacing between the microphones determines the frequency range where the plane wave decomposition will be most accurate. Åbom and Bodén give in [6] a simple criterion that defines the frequency range where the two-microphone method is most accurate.

$$0.1\pi(1 - M^2) < k_0 s < 0.8\pi(1 - M^2) \quad (12)$$

where s is the microphone spacing, M the Mach number, and k_0 the wave-number. Using two times this formula allows to define the spacing between the three microphones, according to the frequency range of interest. In this study where the frequency range of interest is [100 - 5000] Hz, the microphone spacings are chosen to be 17 cm and 2.5 cm.

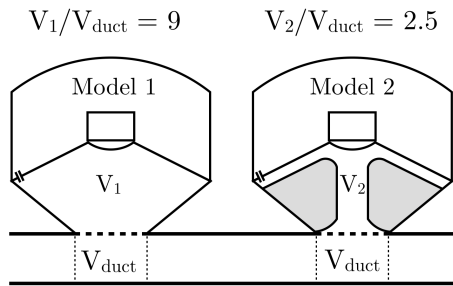
The microphone vent should be located close the front of the microphone, and the microphone holder designed in a way such that the vent is linked to the duct static pressure, and not the atmospheric pressure outside of the duct. Indeed, during measurements with flow, the static pressure in the duct can be different from the atmospheric pressure. A different static pressure at the front and rear of the microphone membrane would alter its sensitivity.

Loudspeakers

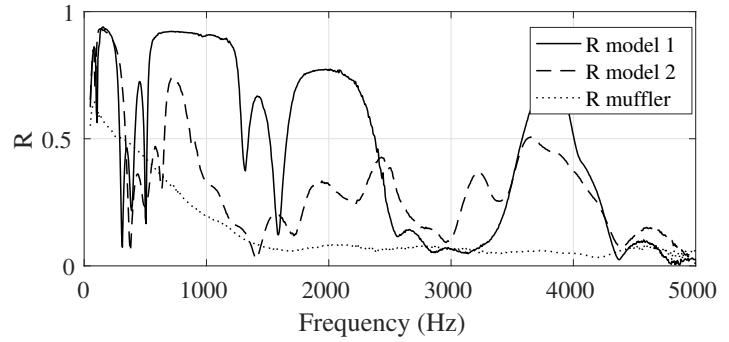
The loudspeakers must be enclosed, and the front and back cavities must be linked by a small pipe: the static pressures at the front and rear of the membrane must be equal. Otherwise, the membrane might be pushed toward its frame, and this would restrain its displacement. The volume of the front cavity (between the speaker membrane and the measurement duct) must be minimized. Otherwise the loudspeakers can account for most of the reflections at the rig termination, as shown in Fig. 3(b). Due to the reflections at the test object and at the rig terminations, for some frequencies a loudspeaker can be located on a pressure node. It will then be impossible to excite the acoustic fields inside the duct with this loudspeaker. This is the reason why three speakers are used on each side. If the ratio of the spacing between loudspeaker I and II, and I and III is an irrational number, all three speakers cannot be on a nodal line at the same time. This guaranties good signal to noise ratio at all frequencies.

Muffler

The mufflers located at the rig terminations have two goals: minimizing the reflections inside the rig and avoiding exterior noise to come into the duct. They are therefore designed to behave as anechoic



(a) Loudspeaker holders, relative volumes



(b) Reflection coefficient magnitude of the rig termination

Figure 3: Rig termination reflection coefficient including the three loudspeakers and the muffler, and reflection coefficient of the sole muffler.

terminations. However, they do not need to be very efficient, since as shown in Fig. 3(b) most of the reflections come from the speakers and not from the muffler.

Overall dimensions

- Distance between the test object and the microphones: this distance should be larger than the characteristic length of the near fields. The near fields (higher order modes that do not propagate) can be considered to have completely decayed at a distance $l_{nf} \approx 3d$ from any discontinuity, where d is the duct diameter. On the outlet side, it should be larger ($\geq 10d$) to allow the flow profile to become fully developed again, as it is disturbed by the fan.
- Distance between the speakers and the microphones: on the inlet side it should be long enough to allow the flow to be fully developed ($\geq 10d$) as the flow profile is disturbed by the speaker perforation, and on the outlet side the minimum length is given by the near fields size ($\geq 3d$).
- Distance between the speakers and the duct termination: this distance can be arbitrary.
- Duct diameter: the duct diameter defines the cut-on frequency, and therefore the higher limit of validity of two-port modelling. Åbom and Bodén showed in [6] that attenuation has to be taken into account to avoid large bias errors in the measurements. The attenuation model that is most widely used for two-port measurements is the one by Dokumaci [8], which takes into account visco-thermal losses but not turbulent losses. The model by Howe [9] includes the latter losses, and can be used to estimate their relative importance. The attenuation coefficient obtained with the Dokumaci and Howe models are compared to each other in Fig. 4, for a 25 mm duct at Mach 0.1.

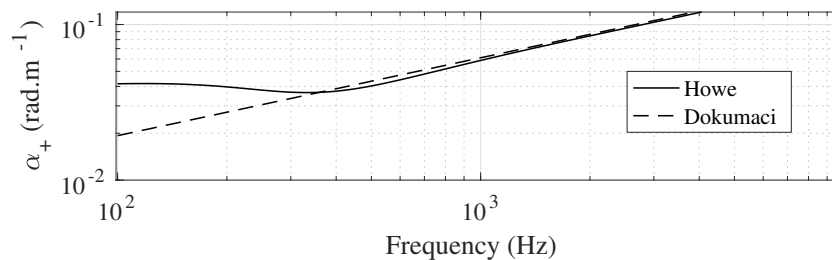


Figure 4: Attenuation coefficient $\alpha_+ = -\mathbf{i}(k_+)$ of planes waves in a 25 mm diameter duct, with Mach number 0.1 (typical values for the fan used in this study).

Turbulent losses appear to dominate over visco-thermal losses below 300 Hz. This means that bias errors will be present in the measurement results below 300 Hz if the attenuation model by Dokumaci is used. In a duct of 35 mm diameter with the same volume flow, turbulent losses dominate only below 100 Hz. To conclude, the duct diameter sets the upper limit of the measurement frequency range, but also the lower limit because of turbulent losses (if the attenuation model by Dokumaci is used).

NEW METHOD FOR SOURCE TERM DETERMINATION

Limitations of the standard method

The standard method becomes singular when the reflections at the rig terminations are high. Indeed, the matrix C in Eq. (9) is computed by inverting the matrix $(T_+(x) + T_-(x)R)$. If this matrix is singular then Eq. (11) is not valid any longer. This can happen only when $|R|$ is close to the identity matrix E , since T_+ or T_- are close to diagonal unit matrices. This means that if the reflection coefficients at the rig terminations are high (R_a and R_b close to one), then the standard method can become singular.

This can be analysed more thoroughly using an error analysis. Let's start from Eq. (9):

$$p_s = Cp \quad \Rightarrow \quad \|C^{-1}p_s\| = \|p\| \quad \Rightarrow \quad \|C^{-1}\|\|\hat{p}_s\| \geq \|p\| \quad (13)$$

Let δp be the error on the measured p . The error on the computed p_s reads:

$$\delta p_s = C\delta p \quad \Rightarrow \quad \|\delta p_s\| \leq \|C\|\|\delta p\| \quad (14)$$

Combining Eqs. (13) and (14) gives:

$$\frac{\|\delta p_s\|}{\|p_s\|} \leq \|C\|\|C^{-1}\| \frac{\|\delta p\|}{\|p\|} \quad \Leftrightarrow \quad \frac{\|\delta p_s\|}{\|p_s\|} \leq \text{cond}(C) \frac{\|\delta p\|}{\|p\|} \quad (15)$$

where $\text{cond}(C)$ is the condition number of the matrix C . It is a real positive number, and $\text{cond}(C) \geq 1$. If C is singular the condition number goes to infinity. And if the condition number is large, then any error on the measured p is amplified when p_s is computed.

Theory of the new post-processing method

To avoid this problem, a new method that makes no explicit use of R_a and R_b is proposed. It does not involve any matrix inversion any more, so it should behave better in cases where R_a and R_b are close to one.

The plane wave decomposition Eq. (2) with over-determination on each side can be rewritten using the pseudo-inverse as:

$$\begin{bmatrix} p_+ \\ p_- \end{bmatrix} = \begin{bmatrix} D_+ \\ D_- \end{bmatrix} \begin{bmatrix} p_1 \\ p_2 \\ p_3 \end{bmatrix} \quad (16)$$

where D_+ and D_- are 1 by 3 vectors (for 3 microphones). Combining the two sides (inlet a and outlet b) into a single equation gives:

$$\begin{bmatrix} p_{a+} \\ p_{b+} \\ p_{a-} \\ p_{b-} \end{bmatrix} = \begin{bmatrix} D_{a+} & 0 \\ 0 & D_{b+} \\ D_{a-} & 0 \\ 0 & D_{b-} \end{bmatrix} \begin{bmatrix} p_{a1} \\ p_{a2} \\ p_{a3} \\ p_{b1} \\ p_{b2} \\ p_{b3} \end{bmatrix} \quad \Leftrightarrow \quad \begin{bmatrix} p_+ \\ p_- \end{bmatrix} = D \begin{bmatrix} p_a \\ p_b \end{bmatrix} \quad (17)$$

The scattering equation at the test object Eq. (1) can be written in matrix form as:

$$\mathbf{p}_s = [\mathbf{E}, -\mathbf{S}] \begin{bmatrix} \mathbf{p}_+ \\ \mathbf{p}_- \end{bmatrix} \quad (18)$$

The source spectrum matrix is finally derived:

$$\mathbf{G}_s = \mathbf{p}_s \mathbf{p}_s^\dagger = [\mathbf{E}, -\mathbf{S}] \mathbf{D} \begin{bmatrix} \mathbf{p}_a \\ \mathbf{p}_b \end{bmatrix} [\mathbf{p}_a^\dagger, \mathbf{p}_b^\dagger] \mathbf{D}^\dagger [\mathbf{E}, -\mathbf{S}]^\dagger \quad (19)$$

$$= [\mathbf{E}, -\mathbf{S}] \mathbf{D} \begin{bmatrix} \mathbf{G}_{aa} & \mathbf{G}_{ab} \\ \mathbf{G}_{ba} & \mathbf{G}_{bb} \end{bmatrix} \mathbf{D}^\dagger [\mathbf{E}, -\mathbf{S}]^\dagger \quad (20)$$

Results

A high speed fan used in Dyson consumer products is measured in the two-port rig described above. Three loudspeakers are mounted on each side, and the holder is the model 1 of Fig. 3(a), i.e. large volume before speaker membrane. The rig reflection coefficient during this measurement is plotted in Fig. 3(b). The Mach number in the duct is $M = 0.05$, and the fan is running at 114 420 RPM. The auto-spectra of the waves emitted towards the inlet $\mathbf{G}_s(1, 1)$ and towards the outlet $\mathbf{G}_s(2, 2)$ are plotted in Fig. 5.

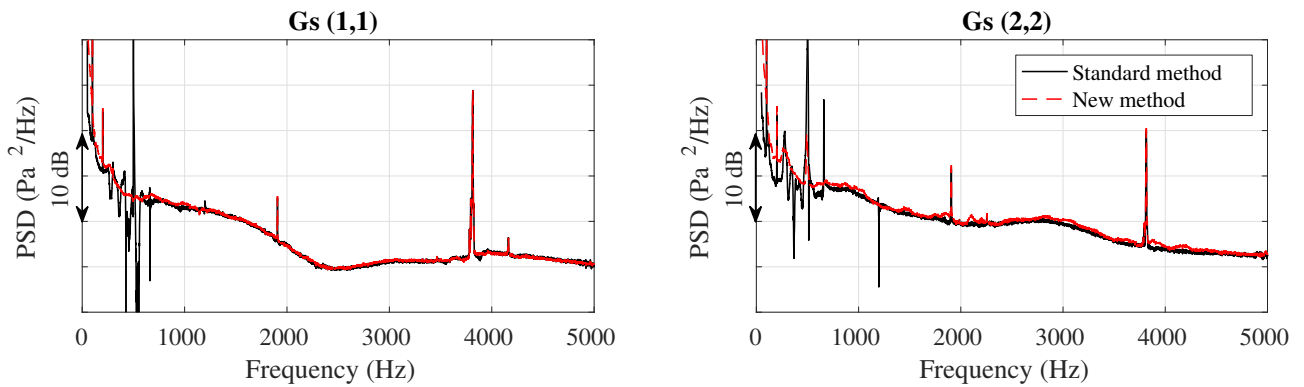


Figure 5: Auto-spectra computed with the standard and the new method, with loudspeaker model 1, see Fig. 3.

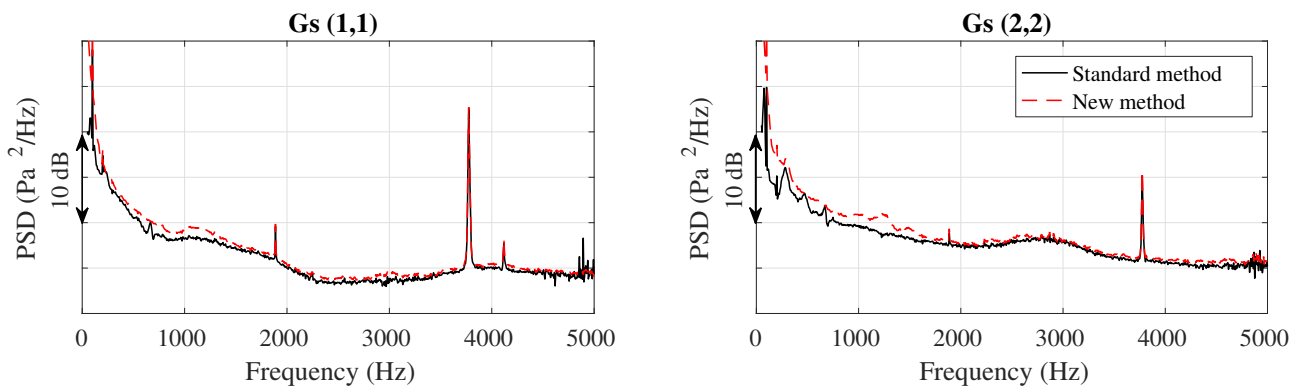


Figure 6: Auto-spectra computed with the standard and the new method, with loudspeaker model 2, see Fig. 3.

The auto-spectra computed with the standard method exhibit large oscillations at low frequencies, around 500 Hz. These are spurious effects that have no physical meaning: the source spectrum is expected in this low frequency range to exhibit a broadband level that varies smoothly. The new method appears to behave much better in this case, as it does not exhibit any large peak or drop in this frequency region.

As shown in Fig. 3b, the loudspeaker model 2 creates much smaller reflections. The auto-spectra obtained in the same test conditions, but replacing the speakers with the model 2 is plotted in Fig. 6. The auto-spectra computed with the standard method are of much better quality, as they vary smoothly with frequency over the whole frequency range. This means that reducing the volume of the loudspeakers front cavities is an efficient solution in avoiding problems due to strong reflections in the rig. In Fig. 6 the new method seems to overestimate slightly the auto-spectra at lower frequencies, below 2000 Hz. This could be due to bad suppression of flow noise. Indeed contrary to the standard method which only uses cross-spectra between microphones separated by more than the flow correlation length, the new method also uses auto-spectra, which are contaminated with flow noise. The hope to suppress flow noise in the new method is that all data is used (cross- and auto-spectra between all microphones, in total 36 spectra), and that this data is projected onto the acoustic fields by the D matrix, see Eq. (20).

To test the sensitivity of the new method to flow noise, uncorrelated white Gaussian noise is added to all microphone signals before the computation of the cross- and auto-spectra. The source spectrum is computed again after this operation, using the modified spectra. This is carried out for different signal to noise ratios, ranging from 30 dB to 0 dB. The source spectra $G_s(1, 1)$ computed with added noise, with the standard and the new method are plotted in Fig. 7.

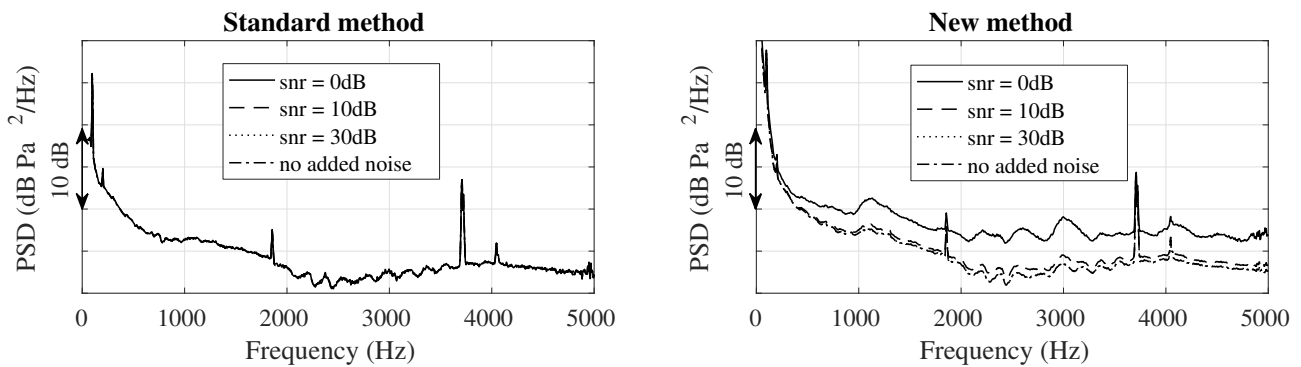


Figure 7: Influence of flow noise on the auto-spectrum of the wave emitted towards inlet side $G_s(1, 1)$.

The new method appears to be quite sensitive to flow noise: the results are completely erroneous if flow noise is as strong as the pressure signals (SNR = 0 dB), and the auto-spectrum is overestimated by 2 dB when SNR = 10 dB. On the other hand the standard method is not sensitive at all to flow noise.

To conclude, the new method that is presented in this paper appears to improve the determination of the source cross-spectrum matrix when the rig reflections are strong. However, it is more sensitive to flow noise than the standard method. Therefore, it is preferable if possible to reduce the rig reflections, by minimizing the loudspeaker volume in order to use the standard method in a case where it is not singular.

VALIDATION

Method

In this section the measured two-port data is compared to sound-power measurements that have been carried out in a duct that complies with the ISO 5136 standard [1], see Fig. 8. In this measurement the terminations of the duct are designed to be anechoic, and the sound pressure level is measured on the inlet and outlet side of the compressor. As there are few reflections in the duct, the measured pressure

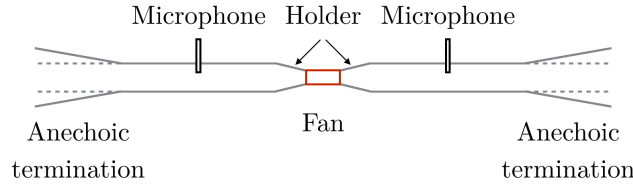


Figure 8: Schematic of the duct for sound power measurements.

is an estimate of the source strength.

A model of the sound-power duct using transfer matrices is built (see Fig. 9), to allow the computation of the sound pressure measured by the microphones, using the two-port of the fan measured in the two-port rig. This provides a validation of the source strength measured in the 2-port rig.

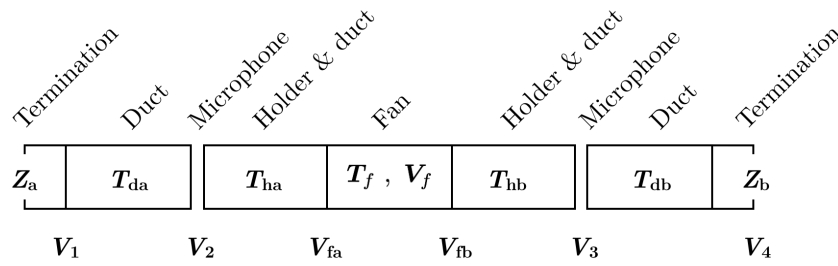


Figure 9: Model of the sound-power duct using two-port theory.

For this case it will be more convenient to use a two-port formulation in the so called transfer-matrix form. For more details of the analysis please refer to Garnell [10]. The microphones are located at sections 2 and 3. $\mathbf{V}_i = \begin{bmatrix} p_i \\ q_i \end{bmatrix}$ are the vectors of state variables (pressure and volume flow), and \mathbf{V}_f is the source term written in the transfer matrix formalism. The microphone pressures are the first components of \mathbf{V}_2 and \mathbf{V}_3 .

First model assuming anechoic terminations

A first computation is carried out to compute the pressure measured by the microphones assuming perfectly anechoic terminations. First, the total two-port of the whole section located between the two microphones is computed. This step involves building an analytic model of the fan holder, and computing the transfer matrix of the duct between the fan and the microphones. The transfer matrices of the different components of the ISO 5136 duct are computed analytically using their geometry as all components are either straight pipes or conical sections.

The relation between the state variables at sections 2 and 3 in Fig. 9 allows to compute the total two-port [10]:

$$\mathbf{V}_2 = \mathbf{T}_{ha} \mathbf{T}_f \mathbf{T}_{hb} \mathbf{V}_3 + \mathbf{T}_{ha} \mathbf{V}_f \quad \Rightarrow \quad \mathbf{T}_{tot} = \mathbf{T}_{ha} \mathbf{T}_f \mathbf{T}_{hb} \quad \mathbf{V}_{tot} = \mathbf{T}_{ha} \mathbf{V}_f \quad (21)$$

For stochastic signals the correct formulation of the source term is the cross-spectrum matrix:

$$\mathbf{T}_{tot} = \mathbf{T}_{ha} \mathbf{T}_f \mathbf{T}_{hb} \quad \mathbf{G}_{tot}^{pq} = \mathbf{T}_{ha} \mathbf{G}_f^{pq} \mathbf{T}_{ha}^\dagger \quad (22)$$

The total two-port is here described in the transfer matrix formalism, but can be converted to the scattering matrix formalism by linear algebra (which is not presented here because it is quite tedious, see [10] for the details). The outcomes of this step are the total scattering matrix \mathbf{S}_{tot} and the total

source spectrum matrix \mathbf{G}_{tot}^s . $\mathbf{G}_{tot}^s(1, 1)$ is the auto-spectrum of the wave emitted towards the inlet side at the cross section 2, and $\mathbf{G}_{tot}^s(2, 2)$ is the auto-spectrum of the wave emitted towards the outlet side at the cross section 3. If there are no reflections, these cross-spectra are those measured by the microphones in the ISO 5136 duct.

Second model taking into account reflections

The real terminations of the ISO 5136 duct are almost certainly not perfectly anechoic. The reflections at the terminations can be taken into account in the model using the two-port formalism. The model of the ISO 5136 duct including terminations has been given in Fig. 9.

The volume flows are all defined positive in the flow direction, that is to say from left to right. The relation between the pressure and volume flow at the terminations is therefore given by:

$$p_1 = -Z_a q_1 \qquad p_4 = Z_b q_4 \qquad (23)$$

where Z_a and Z_b are the radiation impedances. It can be rewritten as:

$$\mathbf{V}_1 = \begin{bmatrix} p_1 \\ q_1 \end{bmatrix} = \begin{bmatrix} 1 \\ -1/Z_a \end{bmatrix} p_1 \qquad \mathbf{V}_4 = \begin{bmatrix} p_4 \\ q_4 \end{bmatrix} = \begin{bmatrix} 1 \\ 1/Z_b \end{bmatrix} p_4 \qquad (24)$$

The equation describing the system of Fig. 9 is:

$$\mathbf{V}_1 = \mathbf{T}_{da} \mathbf{T}_{tot} \mathbf{T}_{db} \mathbf{V}_4 + \mathbf{T}_{da} \mathbf{V}_{tot} \qquad (25)$$

$$\Leftrightarrow \begin{bmatrix} 1 \\ -1/Z_a \end{bmatrix} p_1 = \mathbf{T}_{da} \mathbf{T}_{tot} \mathbf{T}_{db} \begin{bmatrix} 1 \\ 1/Z_b \end{bmatrix} p_4 + \mathbf{T}_{da} \mathbf{V}_{tot} \qquad \Leftrightarrow \mathbf{M} \begin{bmatrix} p_1 \\ p_4 \end{bmatrix} = \mathbf{T}_{da} \mathbf{V}_{tot} \qquad (26)$$

where M is a 2 by 2 matrix whose columns are:

$$\mathbf{M}(:, 1) = \begin{bmatrix} 1 \\ -1/Z_a \end{bmatrix} \qquad \mathbf{M}(:, 2) = \mathbf{T}_{da} \mathbf{T}_{tot} \mathbf{T}_{db} \begin{bmatrix} 1 \\ 1/Z_b \end{bmatrix} \qquad (27)$$

Equation (26) can be solved for p_1 and p_4 by:

$$\begin{bmatrix} p_1 \\ p_4 \end{bmatrix} = \mathbf{M}^{-1} \mathbf{T}_{da} \mathbf{V}_{tot} \qquad \Leftrightarrow \begin{bmatrix} p_1 \\ p_4 \end{bmatrix} = \begin{bmatrix} \mathbf{L}_1 \\ \mathbf{L}_4 \end{bmatrix} \mathbf{T}_{da} \mathbf{V}_{tot} \qquad (28)$$

where \mathbf{L}_1 and \mathbf{L}_4 are the lines of the matrix \mathbf{M}^{-1} .

The vectors \mathbf{V}_1 and \mathbf{V}_4 can then be computed as:

$$\mathbf{V}_1 = \begin{bmatrix} 1 \\ -1/Z_a \end{bmatrix} \mathbf{L}_1 \mathbf{T}_{da} \mathbf{V}_{tot} \qquad \mathbf{V}_4 = \begin{bmatrix} 1 \\ 1/Z_b \end{bmatrix} \mathbf{L}_4 \mathbf{T}_{da} \mathbf{V}_{tot} \qquad (29)$$

The cross-spectrum matrix between the pressure and volume flow is obtained:

$$\mathbf{G}_1^{pq} = \mathbf{V}_1 \mathbf{V}_1^\dagger = \begin{bmatrix} 1 \\ -1/Z_a \end{bmatrix} \mathbf{L}_1 \mathbf{T}_{da} \mathbf{G}_{tot}^{pq} \mathbf{T}_{da}^\dagger \mathbf{L}_1^\dagger \begin{bmatrix} 1 \\ -1/Z_a \end{bmatrix}^\dagger \qquad (30)$$

$$\mathbf{G}_4^{pq} = \mathbf{V}_4 \mathbf{V}_4^\dagger = \begin{bmatrix} 1 \\ 1/Z_b \end{bmatrix} \mathbf{L}_4 \mathbf{T}_{da} \mathbf{G}_{tot}^{pq} \mathbf{T}_{da}^\dagger \mathbf{L}_4^\dagger \begin{bmatrix} 1 \\ 1/Z_b \end{bmatrix}^\dagger \qquad (31)$$

Finally this can be transferred to the microphone sections by the following operation:

$$\mathbf{G}_2^{pq} = \mathbf{T}_{da}^{-1} \mathbf{G}_1^{pq} \mathbf{T}_{da}^{-1\dagger} \qquad \mathbf{G}_3^{pq} = \mathbf{T}_{db} \mathbf{G}_4^{pq} \mathbf{T}_{db}^\dagger \qquad (32)$$

The auto-spectra of the pressures measured by the microphones are $\mathbf{G}_2^{pq}(1, 1)$ and $\mathbf{G}_3^{pq}(1, 1)$. These take into account the reflections at the rig terminations.

Results

As the reflection coefficients of the anechoic terminations are not known, they are simply assumed to be close to $R = 0.2$. The computation including these reflection coefficients must therefore be seen as a qualitative estimation of the influence of end-reflections on the measured sound power.

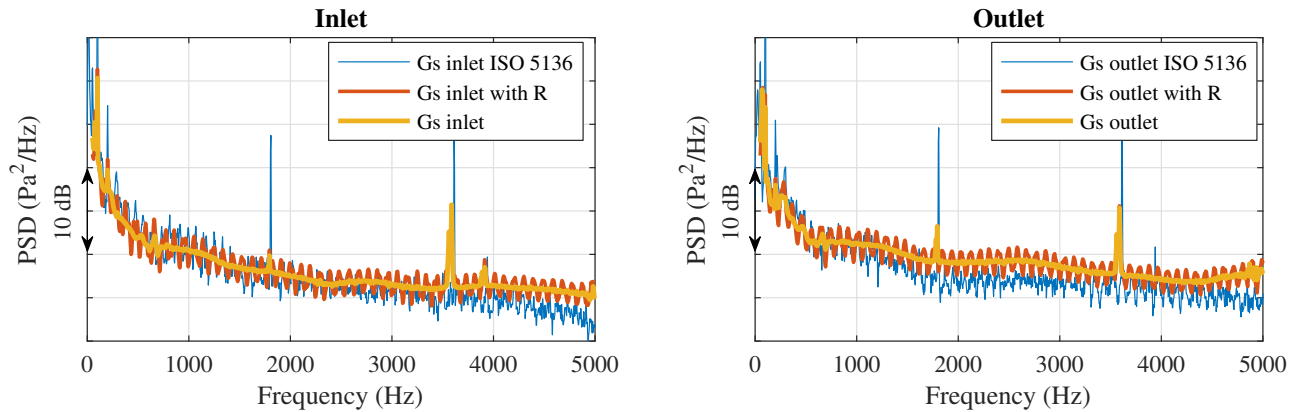


Figure 10: Sound power level measured in the ISO 5136 duct, and computed using the 2-port data of the fan.

Figure 10 shows that the spectra computed using the two-port data are very close to those measured in the ISO 5136 duct. The data from the 2-port, with no reflections taken into account is much smoother. This suggests that the terminations of the ISO 5136 duct are not perfect, and that reflections create the oscillations that can be seen in the measured data. The model with reflections taken into account is also plotted, and it also exhibits oscillations, which are very similar to the measured ones. The amplitude of the oscillations is also very similar, which suggests that the actual reflection coefficient of the ‘anechoic’ terminations is close to $R = 0.2$, even at higher frequencies.

Attenuation during the propagation between the test object and the microphones is taken into account in the two-port model, but not in the ISO 5136 measurement. This may explain the lower level of G_s measured in the ISO duct at higher frequencies. There is also an error in the tone levels (RPM at 1800 Hz, and $2 \times$ RPM at 3600 Hz). This could be due to the fan holder, which is not the same in the ISO duct and in the two-port duct. Experiments at Dyson showed that the mounting of the fan has a large influence on these tone levels.

This comparison with the sound power level measured in the ISO 5136 duct validates the fan source term. However, as there are very few reflections in this system, the influence of the fan scattering is quite small: there are almost no waves that are travelling towards the fan. This measurement provides as a consequence little validation of the fan scattering. To also check the scattering of the fan, this measurement should be repeated but with highly reflective terminations instead of the anechoic terminations.

CONCLUSION AND FURTHER WORK

This study went through the steps of the development of a two-port rig for the measurement of high-speed small fans. The rig was designed after a literature study of the different existing methods for the measurement of two-port models of rotating machines in ducts. The understanding of the physical principles governing the rig behaviour guided the downsizing of existing larger two-port rigs. Turbulent losses have been shown to set a lower limit on the duct diameter. A new post-processing method that works in highly reflective cases has also been tested, but it has been shown to be more sensitive

to flow noise.

The source spectrum has been compared to ISO standard measurements. The measured two-port data and a model of the ISO 5136 duct allowed to predict the pressure measured by the microphones in the ISO duct. An good fit between the ISO and the two-port measurements was found.

One of the next steps in making two-port measurement an efficient tool for product development would be to study the influence of flow rate and fan speed on the scattering matrix and source strength, to derive scaling laws that would allow the prediction of the change in the two-port data when the operating point is changed. The fan two-port at any operating point could then be predicted from measurements at only a few operating points.

REFERENCES

- [1] ISO 5136. *Acoustics – Determination of sound power radiated into a duct by fans and other air-moving devices – In-duct method*, **2003**.
- [2] L. Cremer. *The second annual fairey lecture: The treatment of fans as black boxes*. Journal of Sound and Vibration, 16(1):1–15, **1971**.
- [3] R. Glav and M. Åbom. *A general formalism for analyzing acoustic 2-port networks*. Journal of Sound and Vibration, 202(5):739 – 747, **1997**.
- [4] M. Terao and H. Sekine. *In-duct pressure measurements to determine sound generation, characteristic reflection and transmission factors of an air moving device in air-flow*. In *Proc. of Internoise 1989*, **1989**.
- [5] J. Lavrentjev, M. Åbom, and H. Bodén. *A measurement method for determining the source data of acoustic two-port sources*. Journal of sound and vibration, 183(3):517–531, **1995**.
- [6] M. Åbom and H. Bodén. *Error analysis of two-microphone measurements in ducts with flow*. The journal of the acoustical society of America, 83(6):2429–2438, **1988**.
- [7] A. Holmberg, M. Åbom, and H. Bodén. *Accurate experimental two-port analysis of flow generated sound*. Journal of Sound and Vibration, 330(26):6336–6354, **2011**.
- [8] E. Dokumaci. *A note on transmission of sound in a wide pipe with mean flow and viscothermal attenuation*. Journal of sound and vibration, 208(4):653–655, **1997**.
- [9] M. S. Howe. *The damping of sound by wall turbulent shear layers*. The Journal of the Acoustical Society of America, 98(3):1723–1730, **1995**.
- [10] E. Garnell. *Designing, building and validating a test rig to measure two-port data of small fans*. Master’s thesis, KTH Royal Institute of Technology, **2017**.

ACKNOWLEDGEMENTS

The authors gratefully acknowledge the funding by Dyson, that allowed the realization of this project as a master’s thesis.